28p

N62 17377

NASA TN D-1506

TECHNICAL NOTE

D-1506

STABILITY INVESTIGATION OF A BLUNTED CONE AND A BLUNTED OGIVE WITH A FLARED CYLINDER AFTERBODY AT MACH NUMBERS FROM 0.30 TO 2.85

By Lucille C. Coltrane

Langley Research Center
Langley Station, Hampton, Va.

NATIONAL AERONAUTICS AND SPACE ADMINISTRATION
WASHINGTON

October 1962

NATIONAL AERONAUTICS AND SPACE ADMINISTRATION

TECHNICAL NOTE D-1506

STABILITY INVESTIGATION OF A BLUNTED CONE AND A BLUNTED OGIVE WITH A FLARED CYLINDER AFTERBODY AT MACH NUMBERS FROM 0.30 TO 2.85[1]

By Lucille C. Coltrane

SUMMARY

A cone with a blunt nose tip and a 10.7° half-angle and an ogive with a blunt nose tip and a 20° flared cylinder afterbody have been tested in free flight over a Mach number range from 0.30 to 2.85 and a Reynolds number range from 1×10^6 to 23×10^6. Time histories, cross plots of force and moment coefficients, and plots of the longitudinal-force coefficient, rolling velocity, aerodynamic center, normal-force-curve slope, and dynamic stability are presented. With the center-of-gravity location at about 50 percent of the model length, the models were both statically and dynamically stable throughout the Mach number range. For the cone, the average aerodynamic center moved slightly forward with decreasing speeds and the normal-force-curve slope was fairly constant throughout the speed range. For the ogive, the average aerodynamic center remained practically constant and the normal-force-curve slope remained practically constant to a Mach number of approximately 1.6 where a rising trend was noted. Maximum drag coefficient for the cone, with reference to the base area, was approximately 0.6, and for the ogive, with reference to the area of the cylindrical portion, was approximately 2.1.

INTRODUCTION

Static and dynamic stability characteristics of low-fineness-ratio blunt shapes are required in the design of current reentry bodies. This report presents aerodynamic data from flight tests of two such shapes, a blunted cone with a 10.7° half-angle and a blunted ogive with a 20° flared afterbody. These tests covered a Mach number range from 0.30 to 2.85 and a range of Reynolds number per foot from 1×10^6 to 23×10^6. The free-flight tests were conducted at the NASA Wallops Station.

---

[1]Supersedes recently declassified NASA TM X-199 by Lucille C. Coltrane, 1959.

SYMBOLS

The data are presented relative to the body-axis system and the positive directions of the force coefficients, moment coefficients, and angular velocities are shown in figure 1. The various symbols used throughout this report are defined as follows:

a	accelerometer reading, per g unit
$a_{l,cg}$	longitudinal acceleration, $a_l + \frac{l}{32.2}\left[x\left(\dot{\theta}^2 + \dot{\psi}^2\right)\right]$, per g unit
C_C	longitudinal-force coefficient, $a_{l,cg}\,\frac{W/S}{q}$
C_l	rolling-moment coefficient
C_m	pitching-moment coefficient, $\frac{I_Y}{qSd}\left(\ddot{\theta} - \dot{\psi}\dot{\phi}\right)$
$C_{m_q} + C_{m_{\dot{\alpha}}} = \frac{dC_m}{d\frac{\dot{\theta}d}{2V}} + \frac{dC_m}{d\frac{\dot{\alpha}d}{2V}}$	
C_N	normal-force coefficient, $a_{n,cg}\,\frac{W/S}{q}$
$C_{N_\alpha} = \frac{dC_N}{d\alpha}$	
C_n	yawing-moment coefficient, $\frac{I_Z}{qSd}\left(\ddot{\psi} + \dot{\theta}\dot{\phi}\right)$
C_Y	lateral-force coefficient, $a_{t,cg}\,\frac{W/S}{q}$
d	reference diameter, ft
g	acceleration due to gravity, ft/sec^2
I_X, I_Y, I_Z	moment of inertia about X-, Y-, and Z-axis, respectively, slug-ft^2
l	length of model, ft
M	Mach number
q	dynamic pressure, lb/sq ft

R	Reynolds number per foot
S	reference area of model used in coefficients, sq ft
t	time, sec
V	free-stream velocity, ft/sec
W	weight of model, lb
X,Y,Z	coordinate axes
x	distance from center of gravity, positive forward, ft
x_{ac}	aerodynamic-center position measured from the nose, ft
x_{cg}	center-of-gravity position measured from the nose, ft
α	angle of attack, radians
θ	angle of pitch, radians
λ_0	nonrolling damping constant, 1/sec
$\Delta\lambda$	damping constant due to roll, 1/sec
ϕ	angle of roll, radians
ψ	angle of yaw, radians
ω_0	basic oscillation frequency, radians/sec
$\Delta\omega$	component of total pitch frequency resulting directly from roll, radians/sec
$\ddot{\theta} - \dot{\psi}\dot{\phi}$	effective pitching acceleration, $g\,\frac{a_{n,2} - a_{n,1}}{x_{n,2} - x_{n,1}}$, radians/sec^2
$a_{n,cg}$	normal acceleration, $\frac{a_{n,1}x_{n,2} - a_{n,2}x_{n,1}}{x_{n,2} - x_{n,1}}$, per g unit
$\ddot{\psi} + \dot{\theta}\dot{\phi}$	effective yawing acceleration, $g\,\frac{a_{t,2} - a_{t,1}}{x_{t,2} - x_{t,1}}$, radians/sec^2
$a_{t,cg}$	transverse acceleration, $\frac{a_{t,1}x_{t,2} - a_{t,2}x_{t,1}}{x_{t,2} - x_{t,1}}$, per g unit

Subscripts:

l	longitudinal
n	normal
t	transverse
1	forward end of model
2	rear end of model

A dot above a symbol indicates time rate of change of symbol.

MODELS

The physical characteristics of the models are presented in table I. Drawings of the models are shown in figure 2 and photographs are presented in figure 3.

The cone model of fineness ratio 2.1 had a blunt nose tip and a 10.7° flared body. The ogive model of fineness ratio 3.6 had a blunt nose tip and a 20° flared cylinder afterbody. The center of gravity for each model was located at approximately 50 percent of the model length. Each model contained three small pulse rockets to give a lateral disturbance. These pulse rockets were mounted near the base, equally spaced around the model perimeter and normal to the longitudinal axis.

INSTRUMENTATION

Model instrumentation consisted of an NASA six-channel telemeter which transmitted data from five accelerometers and one roll-rate gyro located as follows: The roll-rate gyro, the longitudinal accelerometer, one normal and one transverse accelerometer in the forward end of the model and one normal and one transverse accelerometer in the rear of the model. Ground instrumentation included a CW Doppler radar unit to measure the velocity of the model, a modified SCR 584 tracking radar set to determine the flight path, and a rollsonde receiver used as an additional measure of the rolling velocity. Fixed and tracking motion-picture cameras were used to observe the model during the first portion of the flight. Atmospheric data were obtained from a rawinsonde released near firing time.

TESTS AND ANALYSIS

The models were ground launched at an angle of 70° from the horizontal by means of a zero length launcher. A solid-propellant XM19 (Recruit) rocket motor boosted the models to maximum velocity.

A photograph of the model-booster arrangement is shown in figure 3. The conical flare on the booster was used to provide stability and enough inherent fixed drag to separate the booster from the model. The model was held to the booster by a bolt which breaks in tension through a piston arrangement driven by gas from a powder charge during the booster portion of the flight. When the ogive model was disturbed at separation and by the firing of a pulse rocket, the instruments exceeded their calibrated ranges for a short while. Thus, for this model the peak Mach number range for data purposes was reduced.

Data obtained from normal and transverse accelerometers located at two positions in the model were used to determine the pitching-moment and yawing-moment coefficients. The methods of analysis presented in references 1 and 2 were used for reducing these data. Before determining the damping coefficients, the amplitudes of the oscillations were corrected for the effect of the decreasing dynamic pressure. (See ref. 3.) Applying this correction caused an increase in the values of $C_{m_q} + C_{m_{\dot{\alpha}}}$ of about 14 percent for the cone model and about 22 percent for the ogive model compared with the values that would have been obtained if no correction had been applied. The values used to determine C_{N_α} and $C_{m_q} + C_{m_{\dot{\alpha}}}$ are presented in table II.

ACCURACY

The accuracy of the data obtained, based on a maximum instrument inaccuracy estimated to be ±2 percent of the calibrated range, is as follows:

Coefficient	Cone model at Mach number of -			Ogive model at Mach number of -		
	2.85	1.03	0.32	1.86	1.53	0.64
C_N	±0.001	±0.013	±0.179	±0.011	±0.017	±0.113
C_Y	±.001	±.013	±.182	±.011	±.016	±.111
C_C	±.006	±.059	±.842	±.049	±.075	±.504

PRESENTATION OF RESULTS

The variation of test Reynolds number per foot with test Mach number is presented in figure 4. The model flight paths are presented as the variation of altitude with horizontal distance in figure 5, and the variations of velocity and dynamic pressure with time are shown in figure 6.

Time histories of the normal-force coefficient, lateral-force coefficient computed at the center of gravity, and Mach number are presented in figures 7 and 8. Basic-data cross plots of force and moment coefficients are shown in figures 9 and 10. The rolling velocity is shown as a function of Mach number in figure 11. The variation with Mach number of the average aerodynamic center, the normal-force-curve slope, the dynamic stability, and the measured longitudinal-force coefficient is presented in figures 12 and 13.

DISCUSSION OF RESULTS

Time History

The time histories of C_Y and C_N show the motion of the models caused by the separation from the booster rocket motor and by the firing of the three pulse rockets. When disturbed, both models experienced a coupled motion with respect to the body-axis system and damping of the oscillations throughout the flight.

Basic-Data Plots

Cross plots of C_N and C_Y presented in figures 9 and 10 for various Mach numbers indicate the model motion. The trim center was estimated and a time history of the resultant force vector was obtained which was used to determine the values given in table II. The angular displacement of adjacent peaks on the cross plots gives an indication of the rolling rate of the models, and the values obtained are shown in figure 11 with measured averages from the rollsonde and roll-rate-gyro data.

Pitching- and yawing-moment coefficients as a function of force coefficients are shown in figures 9 and 10 for various Mach numbers. These variations show a stable slope which is linear throughout the speed range.

Aerodynamic Characteristics

The normal-force, longitudinal-force, and stability characteristics plotted against Mach number are shown for the cone and ogive models in figures 12 and 13, respectively. Also included in figure 12 are data for a 10° half-angle cone of reference 4, data for a 7.5° half-angle cone of references 5 and 6 and some unpublished data for a 7.5° half-angle cone. The models were both statically

and dynamically stable throughout the Mach number range about a point located approximately 50 percent of the body length.

For the cone (fig. 12), the average aerodynamic center moved slightly forward with decreasing speeds, and the normal-force-curve slope was fairly constant throughout the speed range. The reference theoretical and experimental cone data showed good agreement with the data of this test. It is seen that the maximum longitudinal-force-coefficient value is approximately 0.60 with reference to maximum diameter.

The average aerodynamic center for the ogive model (fig. 13) remained practically constant throughout the speed range. The test points for the normal-force-curve slope show little change throughout the speed range for this model except for the point at $M = 1.86$. The trend of this value approaches the estimated theoretical values. However, because of the rapid change in the basic oscillation frequency ω_0, as can be seen from the time-history plot (fig. 8), it should be treated as a qualitative value. Theoretical estimates were also made for the aerodynamic-center location. These estimates are based on second-order shock-expansion theory for the ogive-cylinder (ref. 7) and conical flow over the surface of the flare. Maximum drag coefficient, based on the diameter of the cylindrical portion of the model, was approximately 2.1.

SUMMARY OF RESULTS

From flight tests, over a Mach number range from 0.30 to 2.85 and a Reynolds number range from 1×10^6 to 23×10^6, of a fineness-ratio-2.1 blunted cone with a 10.7° half-angle and a fineness-ratio-3.6 blunted ogive with a 20° flared afterbody, the following results were obtained:

1. The models were both statically and dynamically stable throughout the Mach number range with the center of gravity located at approximately 50 percent of the body length. For the cone, the average aerodynamic center moved slightly forward with decreasing speeds and the normal-force-curve slope remained fairly constant throughout the speed range. Good agreement with theory was obtained. For the ogive, the average aerodynamic center remained practically constant and agreed well with theory. The normal-force-curve slope was practically constant throughout the speed range except at a Mach number of 1.86; this value approached the estimated theoretical values.

2. The maximum drag coefficient of the cone model, with reference to the diameter of the base, was approximately 0.60 and of the ogive model, with reference to the diameter of the cylindrical portion, was approximately 2.1.

Langley Research Center,
National Aeronautics and Space Administration,
Langley Field, Va., August 24, 1959.

REFERENCES

1. Coltrane, Lucille C.: Investigation of Two Bluff Shapes in Axial Free Flight Over a Mach Number Range From 0.35 to 2.15. NACA RM L58A16, 1958.

2. Nelson, Robert L.: The Motions of Rolling Symmetrical Missiles Referred to a Body-Axis System. NACA TN 3737, 1956.

3. Friedrich, Hans R., and Dore, Frank J.: The Dynamic Motion of a Missile Descending Through the Atmosphere. Jour. Aero. Sci., vol. 22, no. 9, Sept. 1955, pp. 628-632, 638.

4. Tobak, Murray, and Wehrend, William R.: Stability Derivatives of Cones at Supersonic Speeds. NACA TN 3788, 1956.

5. Fisher, Lewis R., and DiCamillo, Joseph R.: Investigation of Several Blunt Bodies To Determine Transonic Aerodynamic Characteristics Including Effects of Spinning and of Extendible Afterbody Flaps and Some Measurements of Unsteady Base Pressures. NASA MEMO 1-21-59L, 1959.

6. Letko, William: Experimental Investigation at a Mach Number of 3.11 of the Lift, Drag, and Pitching-Moment Characteristics of a Number of Blunt Low-Fineness-Ratio Bodies. NASA MEMO 1-18-59L, 1959.

7. Syvertson, Clarence A., and Dennis, David H.: A Second-Order Shock-Expansion Method Applicable to Bodies of Revolution Near Zero Lift. NACA Rep. 1328, 1957. (Supersedes NACA TN 3527.)

TABLE I

PHYSICAL CONSTANTS FOR MODELS TESTED

Constant	Cone	Ogive
W, lb	83.5	85.0
I_X, slug-ft^2	.211	.218
I_Y, slug-ft^2	1.387	1.505
I_Z, slug-ft^2	1.387	1.505
x_{cg}/l	.495	.496
d (ref.), ft	1.167	.667
l, ft	2.458	2.371
S, sq ft	1.070	.348

TABLE II

VALUES USED TO DETERMINE SLOPE OF NORMAL-FORCE

COEFFICIENTS AND DYNAMIC STABILITY

Mach number	ω_0	λ_0	$\Delta\lambda$	$\Delta\omega$	$\frac{\frac{I_X}{I_Y}\left(1 - \frac{I_X}{4I_Y}\right)}{\left(1 - \frac{I_X}{2I_Y}\right)^2}$	$\frac{dC_m}{dC_N}$ or $\frac{dC_n}{dC_Y}$
Cone						
2.85	72.5	-4.75	0	-4.5	0.171	-0.34
2.47	58.7	-2.89	0	-3.0	.171	-.32
2.06	50.0	-3.98	0	-3.0	.171	-.30
1.03	20.7	-1.57	0	-1.0	.171	-.29
.88	17.0	-1.00	0	-1.0	.171	-.24
.32	4.6	-.34	0	-1.0	.171	-.20
Ogive						
1.86	[a]27.7	(b)	(b)	-1.0	0.163	-0.25
1.53	18.0	-1.63	0	-1.0	.163	-.20
.81	10.0	-.61	0	-1.5	.163	-.23
.64	6.5	-.36	0	-.7	.163	-.18

[a]Qualitative value.

[b]Reliable value was not obtained.

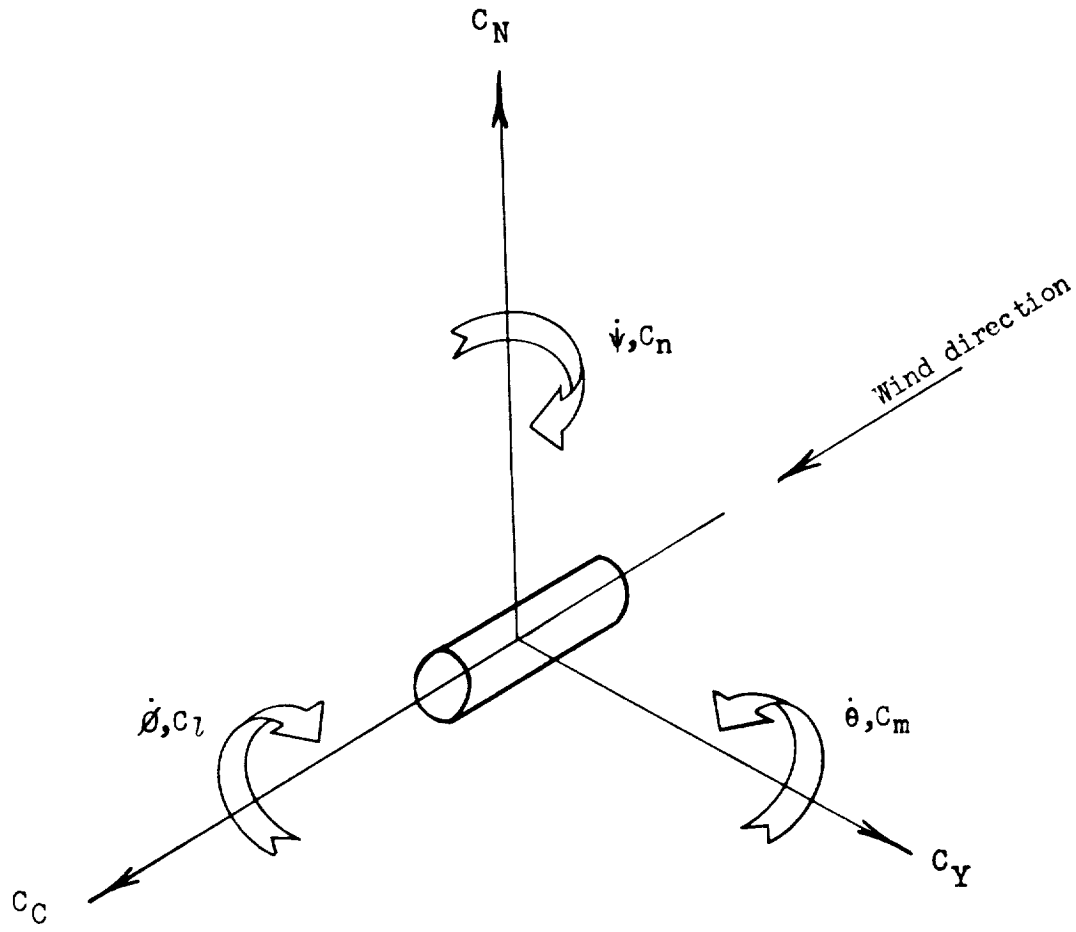

Figure 1.- Axes system with origin at center of gravity. Positive directions of force and moment coefficients and angular velocities are indicated by the arrows.

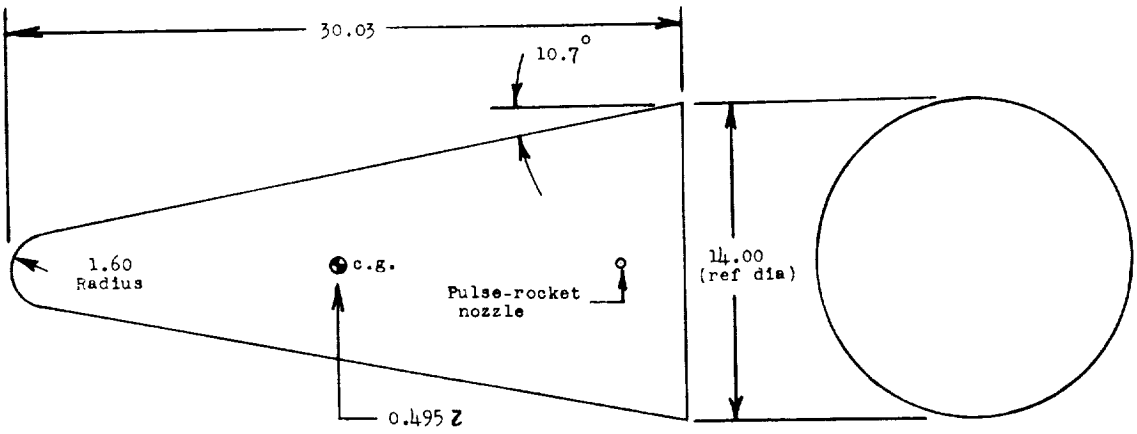

(a) Cone model.

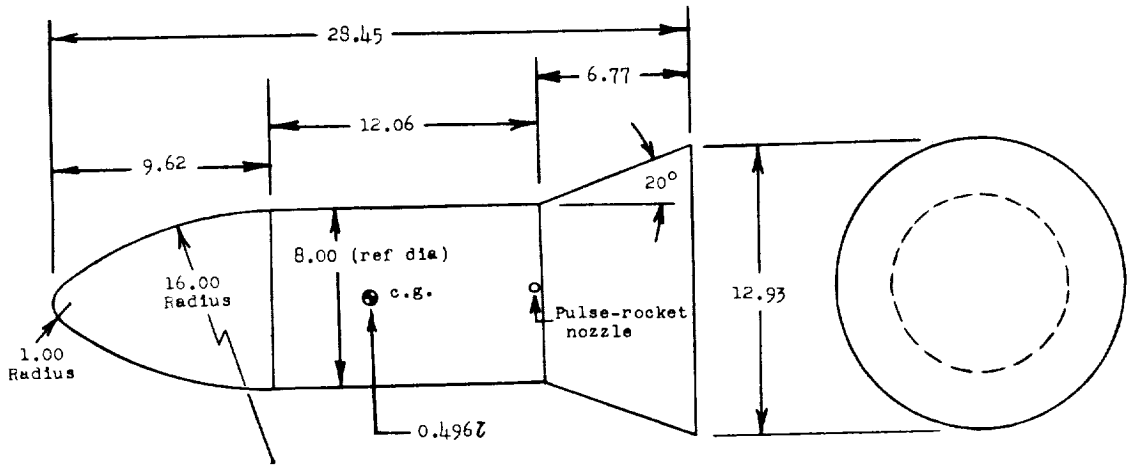

(b) Ogive model.

Figure 2.- Drawings of models tested. All dimensions are in inches.

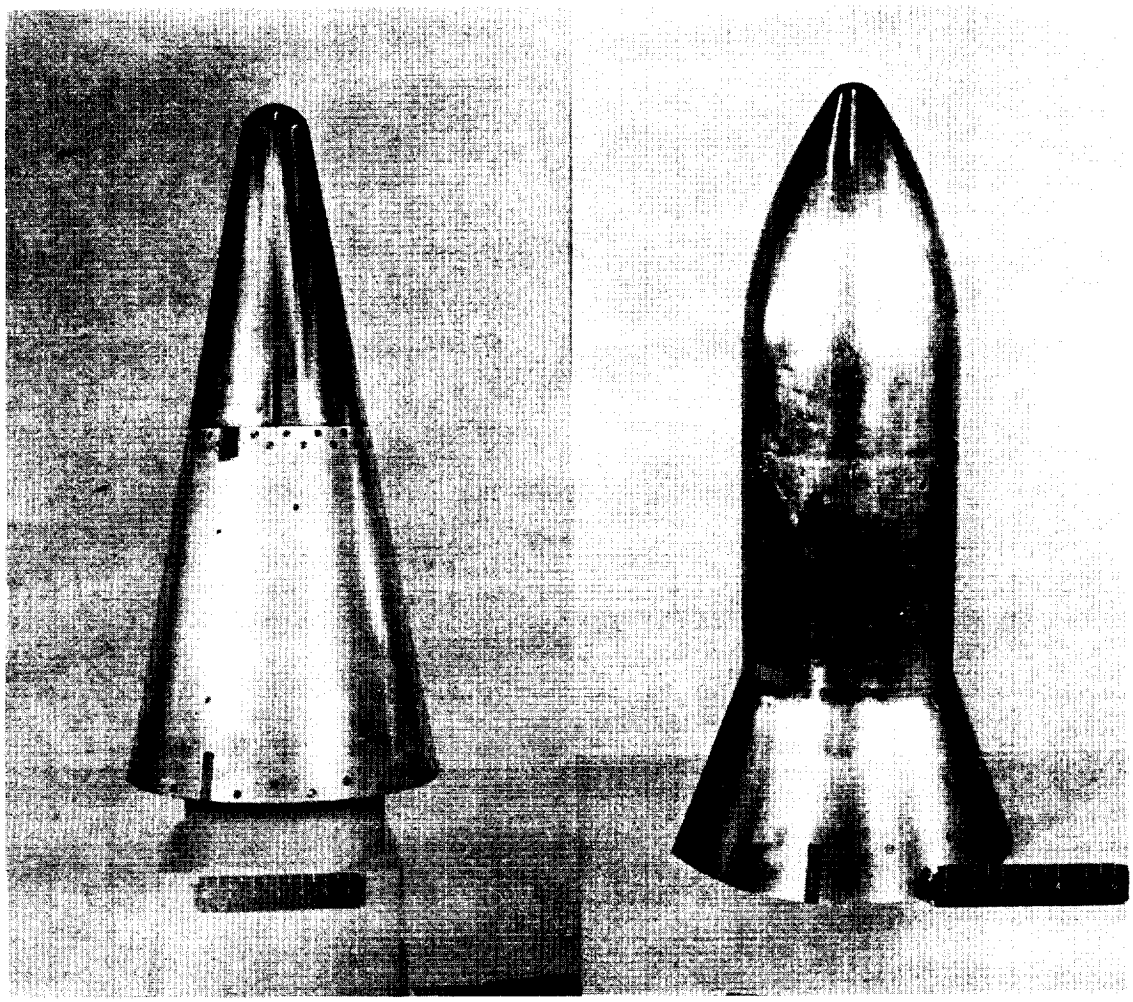

(a) Cone model. (b) Ogive model.

Figure 3.- Photographs of models tested. L-59-6018

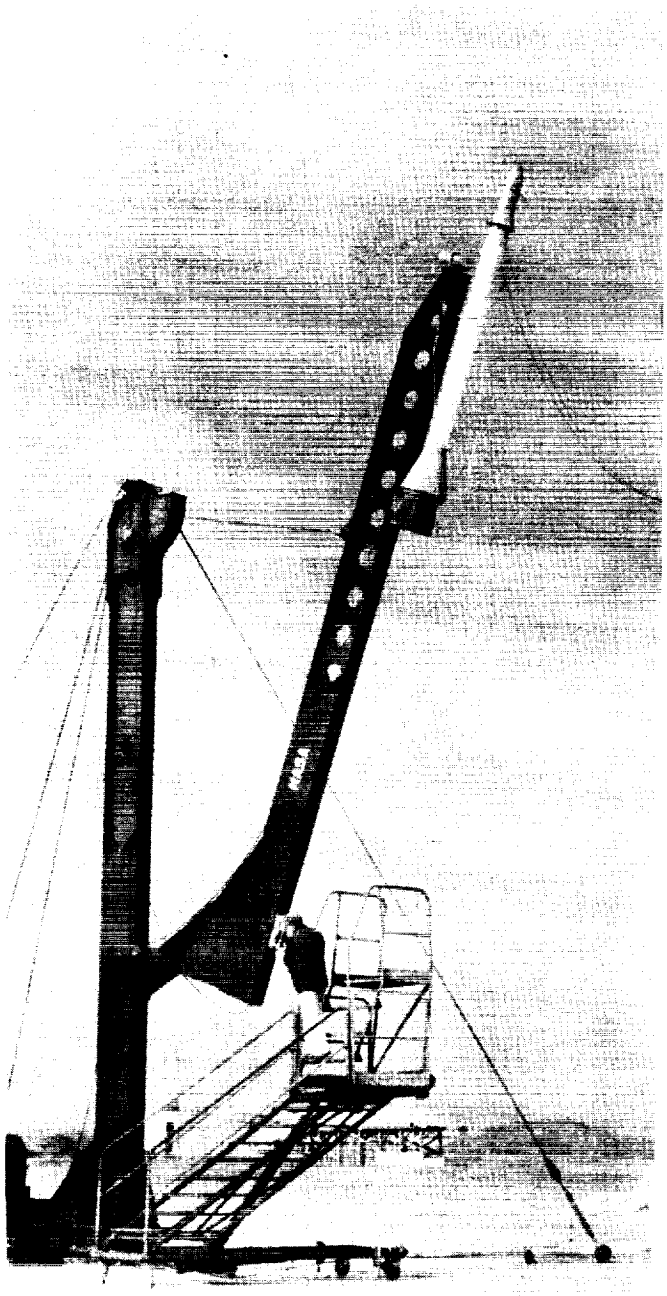

(c) Ogive model on booster in launching position. L-59-714

Figure 3.- Concluded.

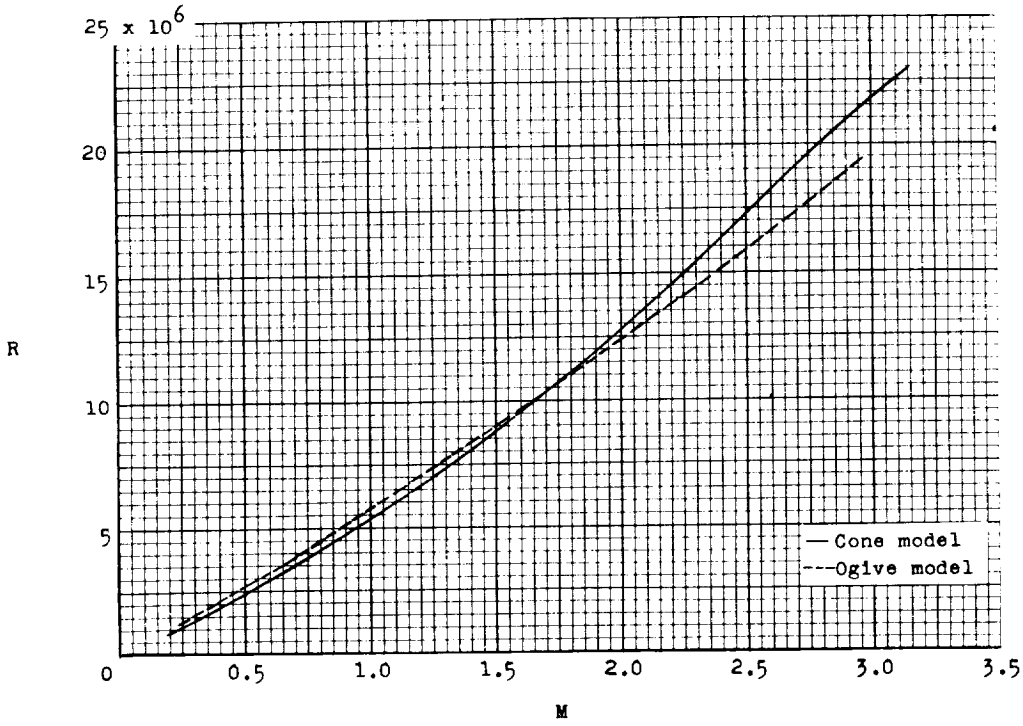

Figure 4.- Test Reynolds number per foot.

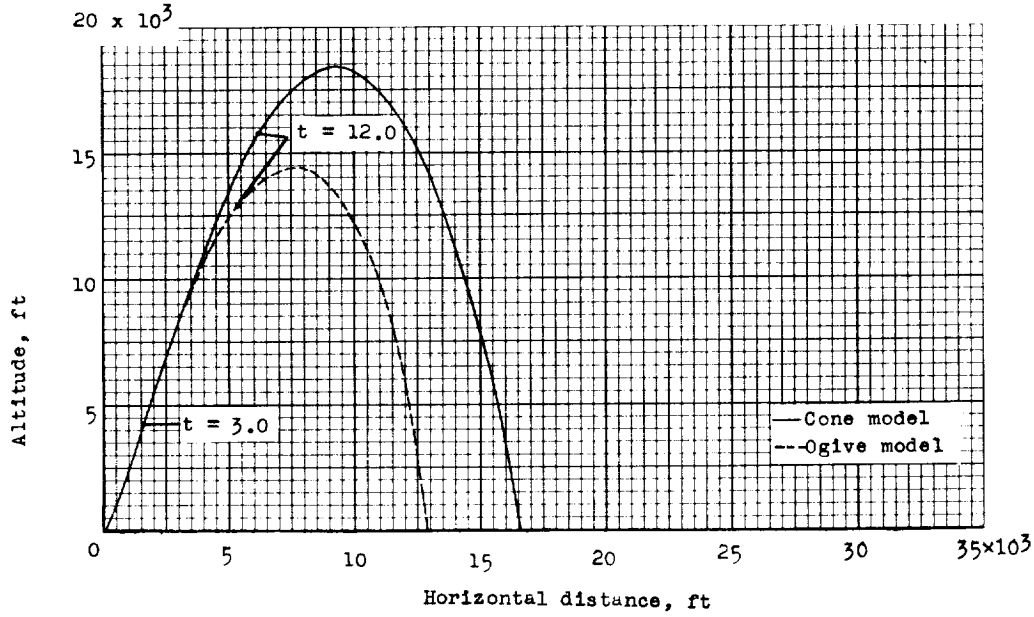

Figure 5.- Flight paths of models tested.

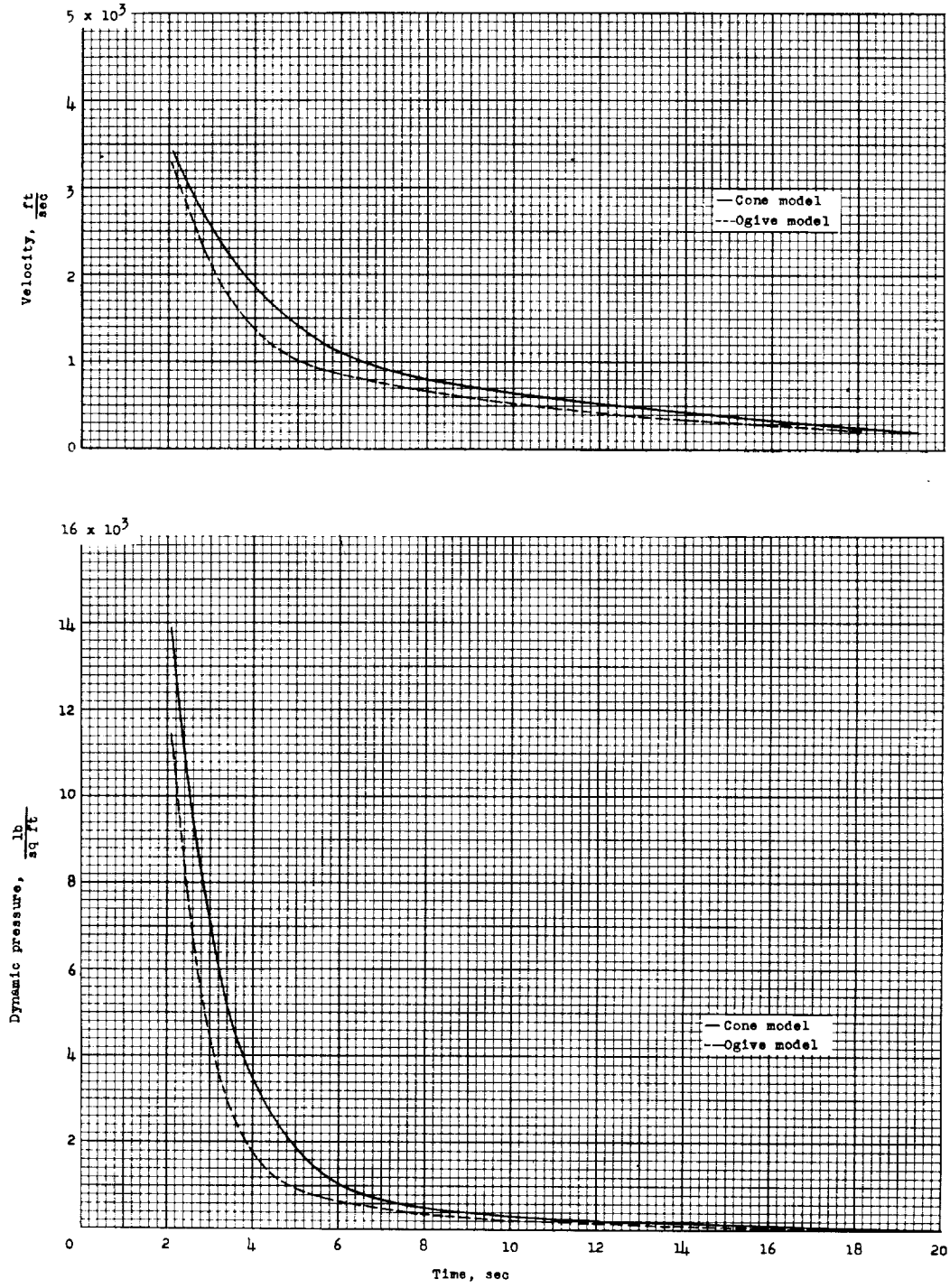

Figure 6.- Velocity and dynamic pressure of models tested.

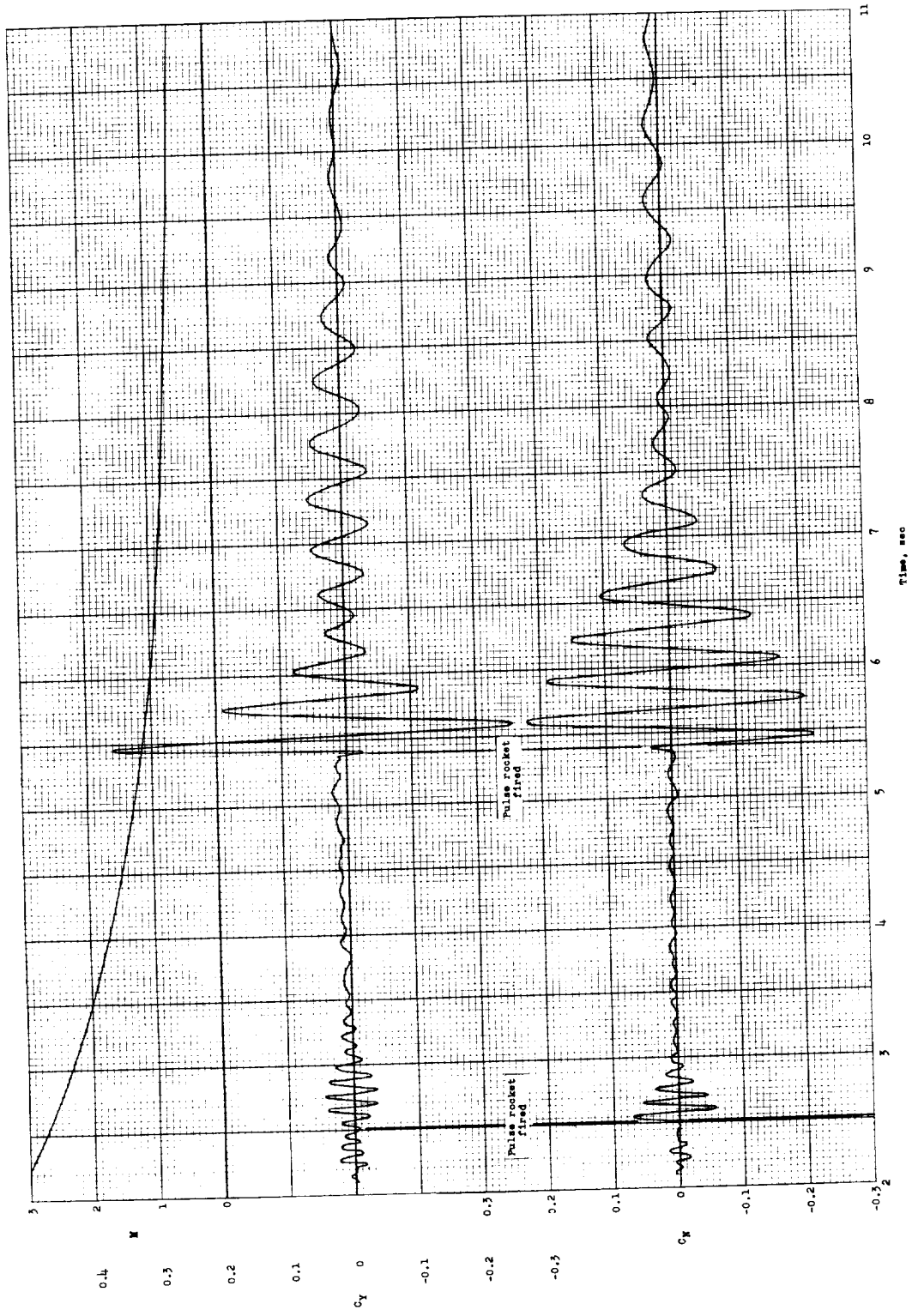

Figure 7.- Time history of cone model.

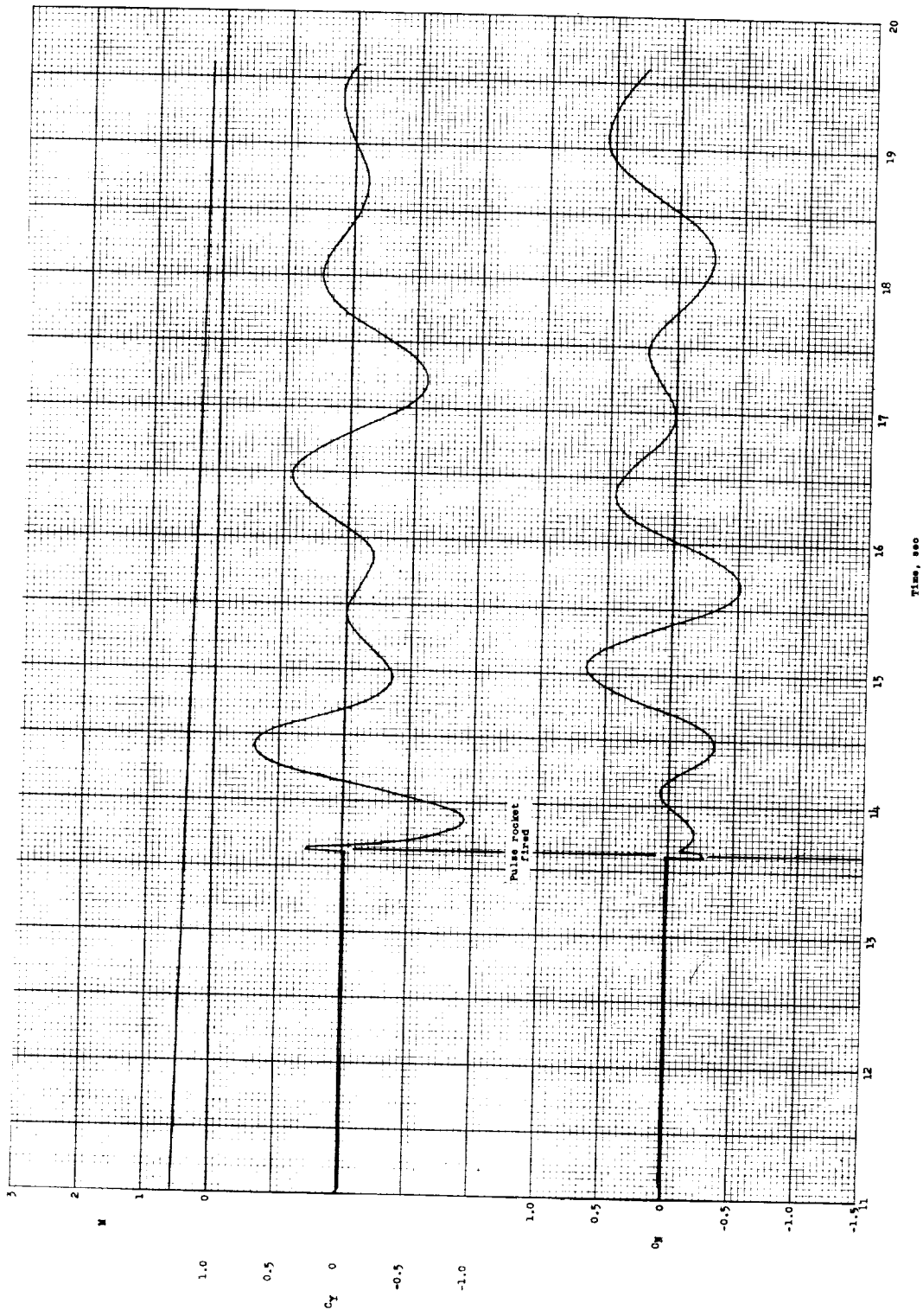

Figure 7.- Concluded.

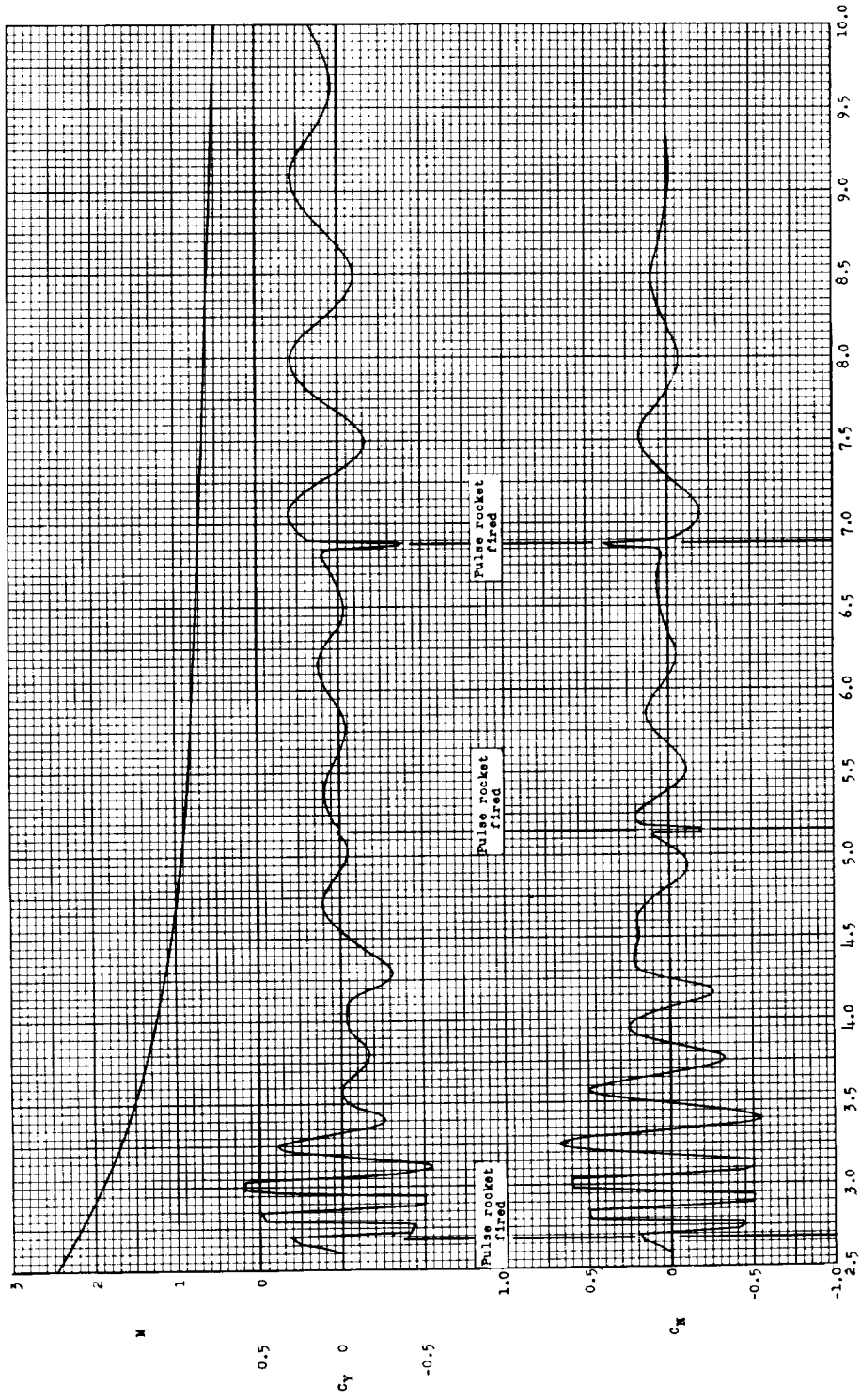

Figure 8.- Time history of ogive model.

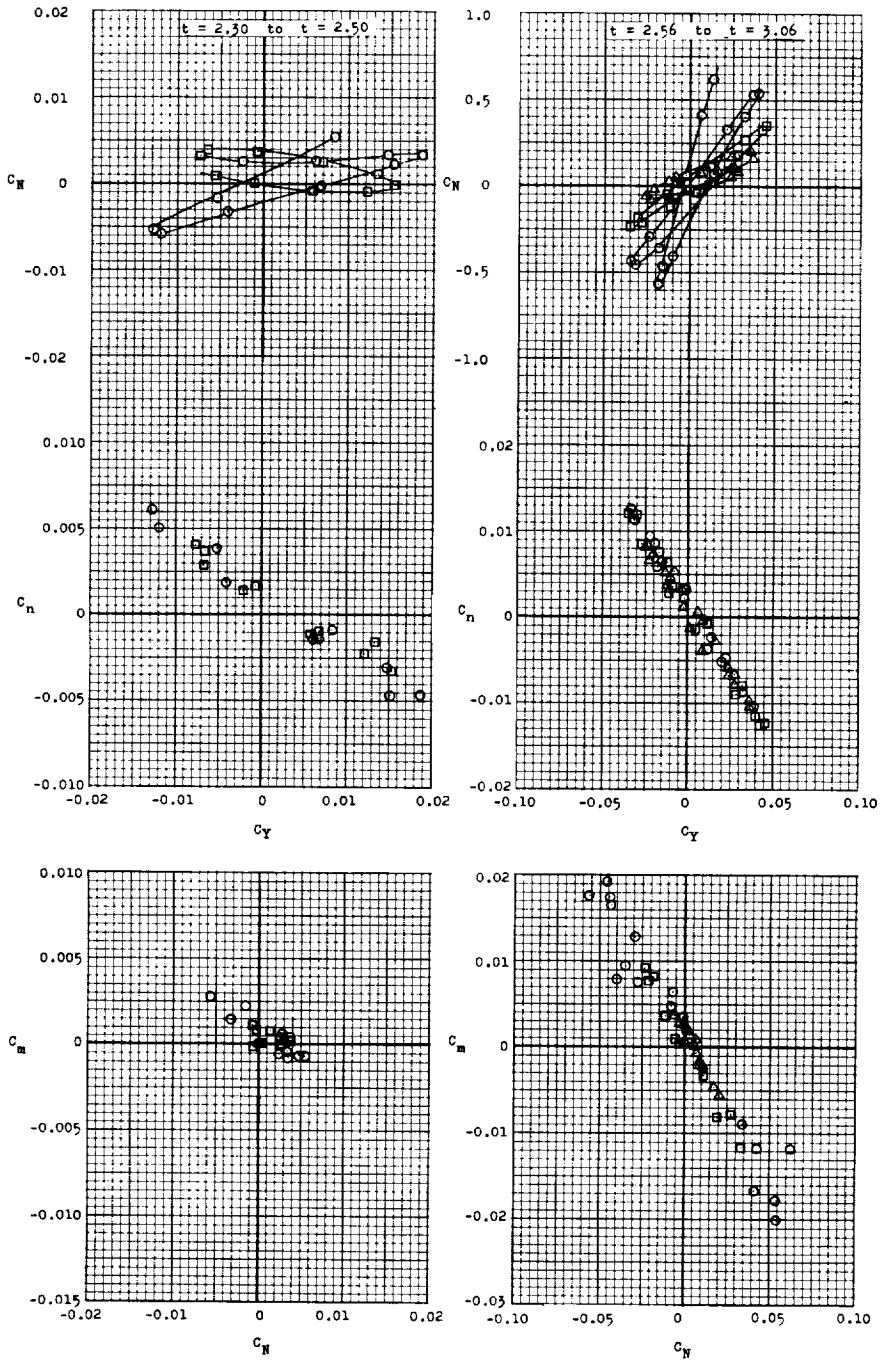

(a) M = 2.95 to M = 2.75. (b) M = 2.68 to M = 2.26.

Figure 9.- Basic-data cross plots of force and moment coefficients. Cone model. The time sequence is indicated by the symbols ⊙, ⊡, △.

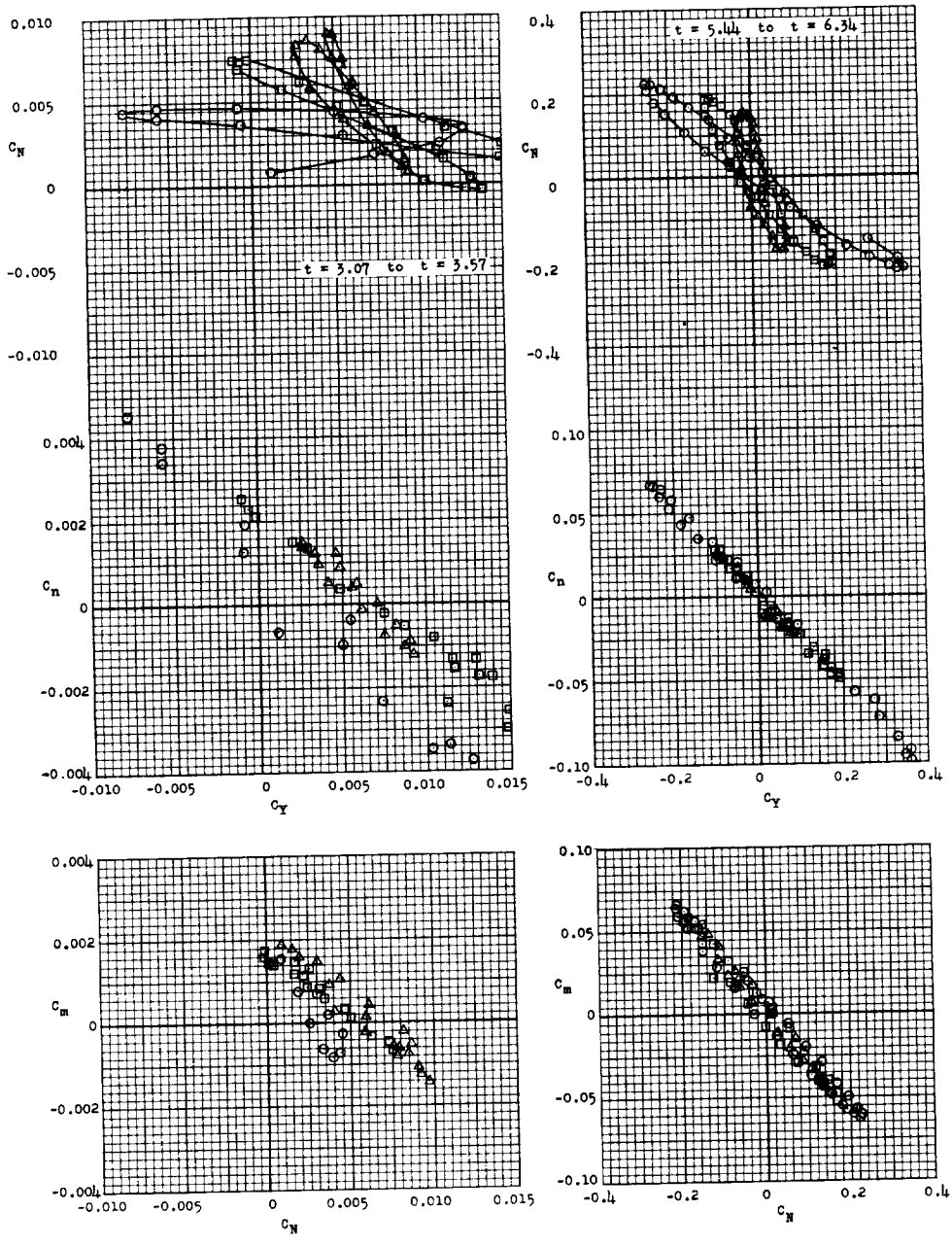

(c) M = 2.27 to M = 1.95.

(d) M = 1.17 to M = 0.93.

Figure 9.- Continued.

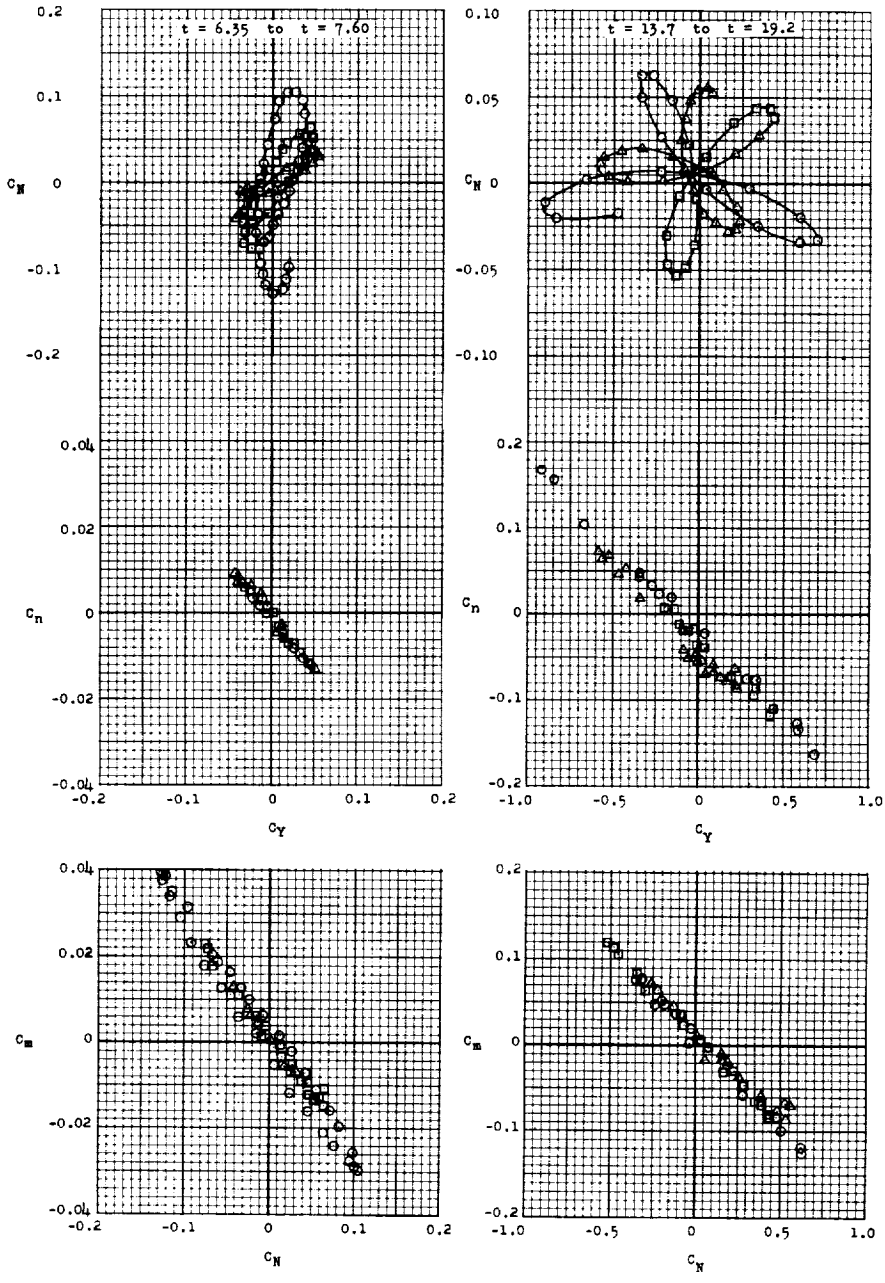

(e) M = 0.93 to M = 0.78. (f) M = 0.42 to M = 0.21.

Figure 9.- Concluded.

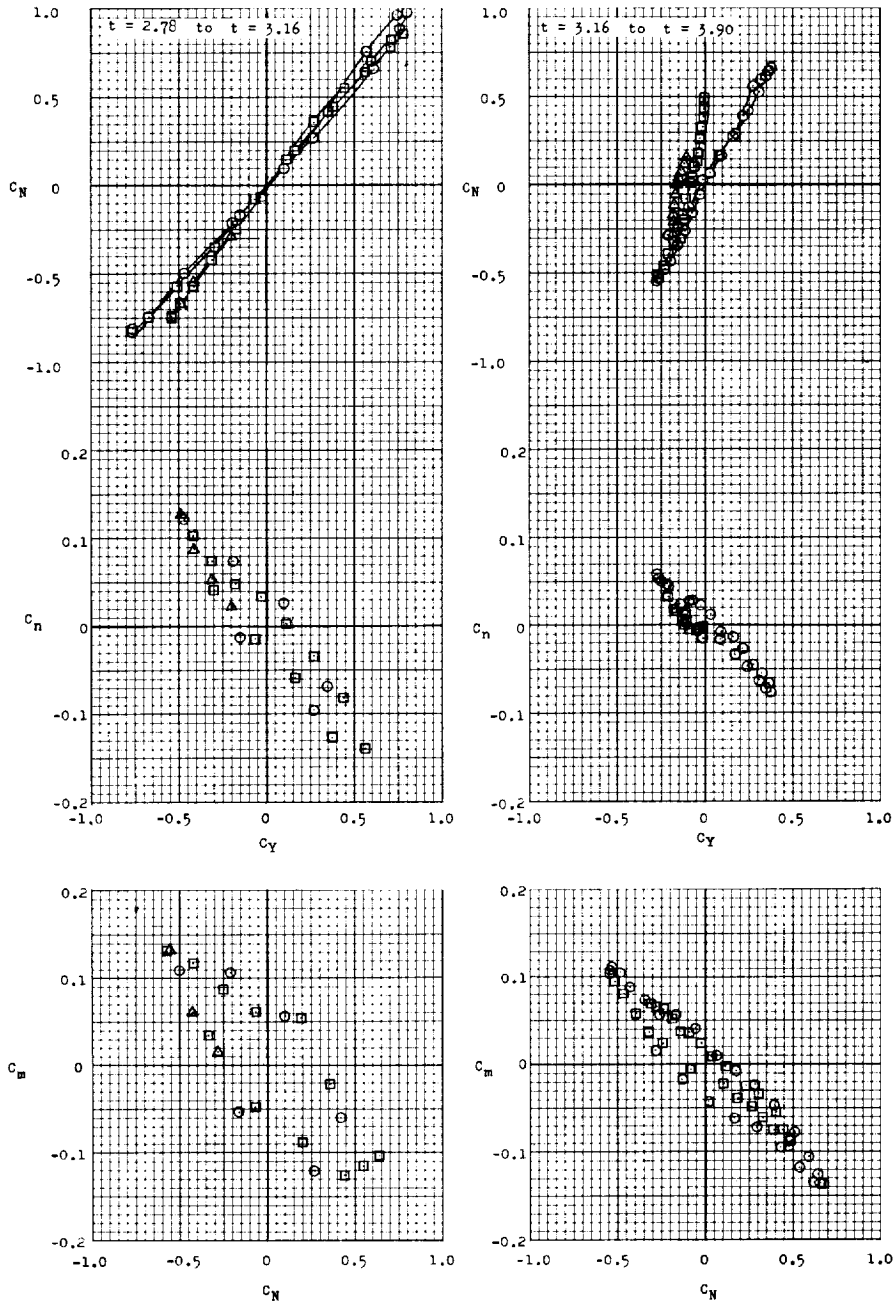

(a) M = 2.14 to M = 1.77. (b) M = 1.77 to M = 1.30.

Figure 10.- Basic-data cross plots of force and moment coefficients. Ogive model. The time sequence is indicated by the symbols ⊙, ⊡, and △.

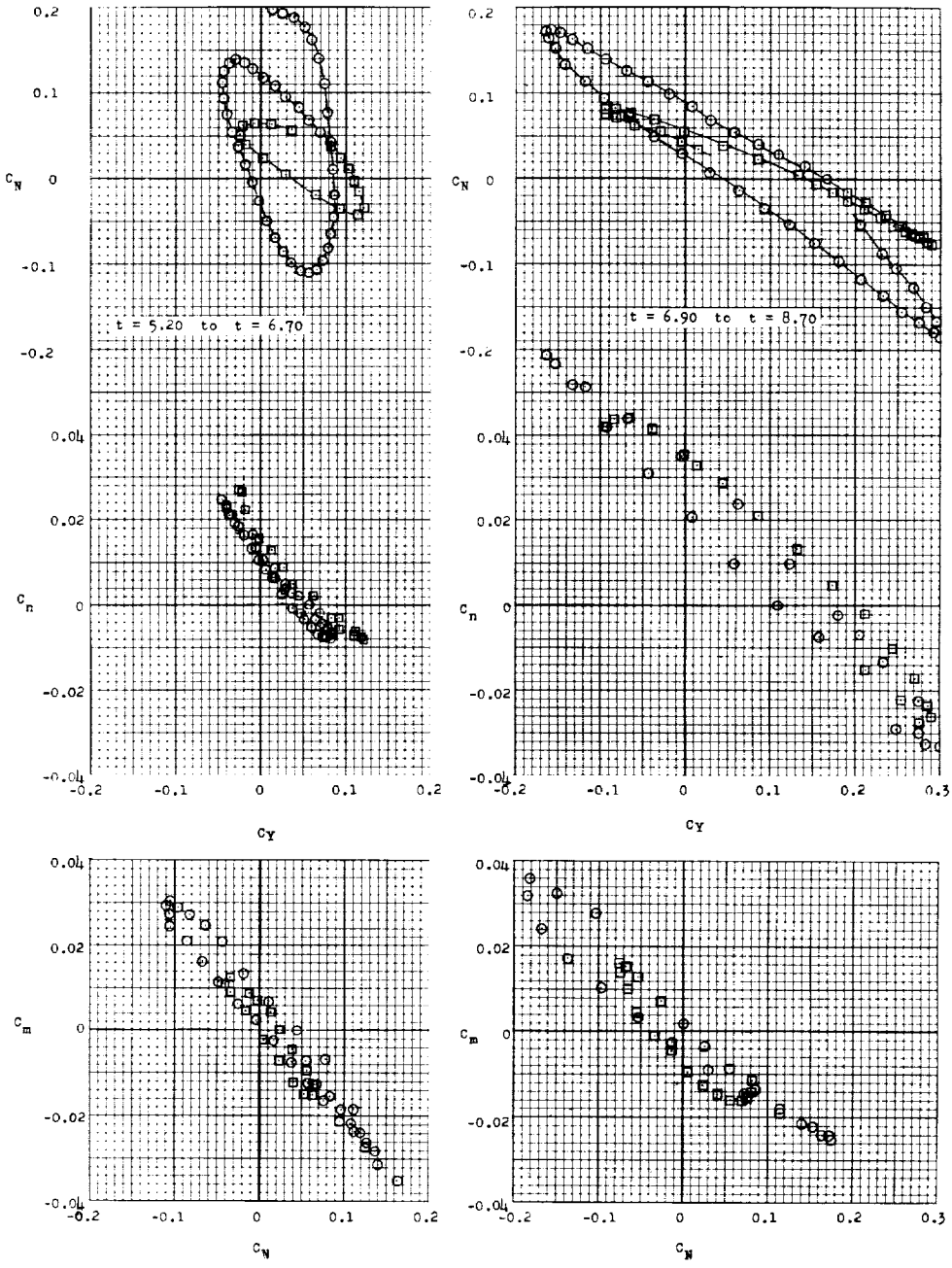

(c) M = 0.90 to M = 0.72. (d) M = 0.70 to M = 0.56.

Figure 10.- Concluded.

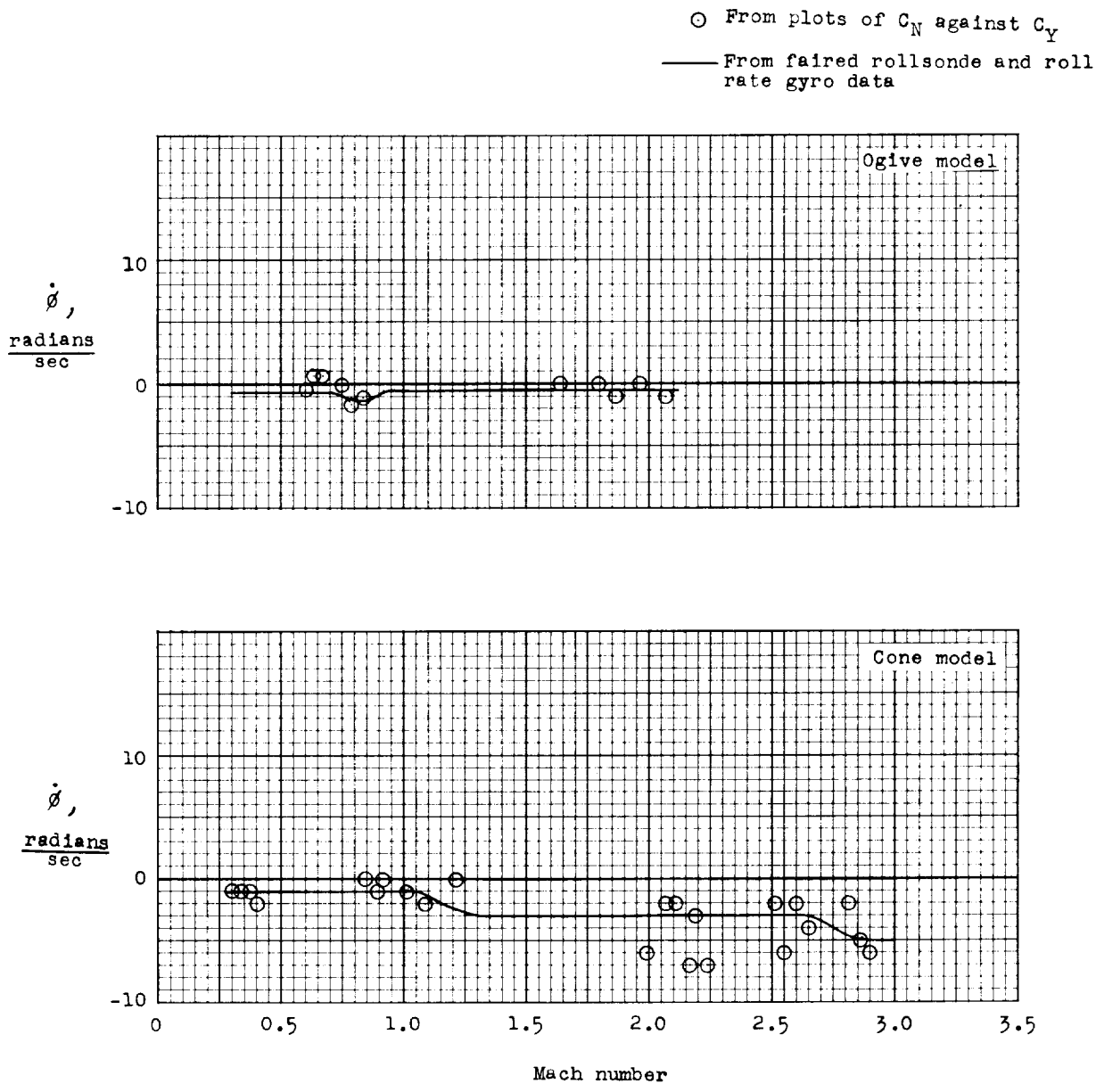

Figure 11.- Variation of rolling velocity with Mach number.

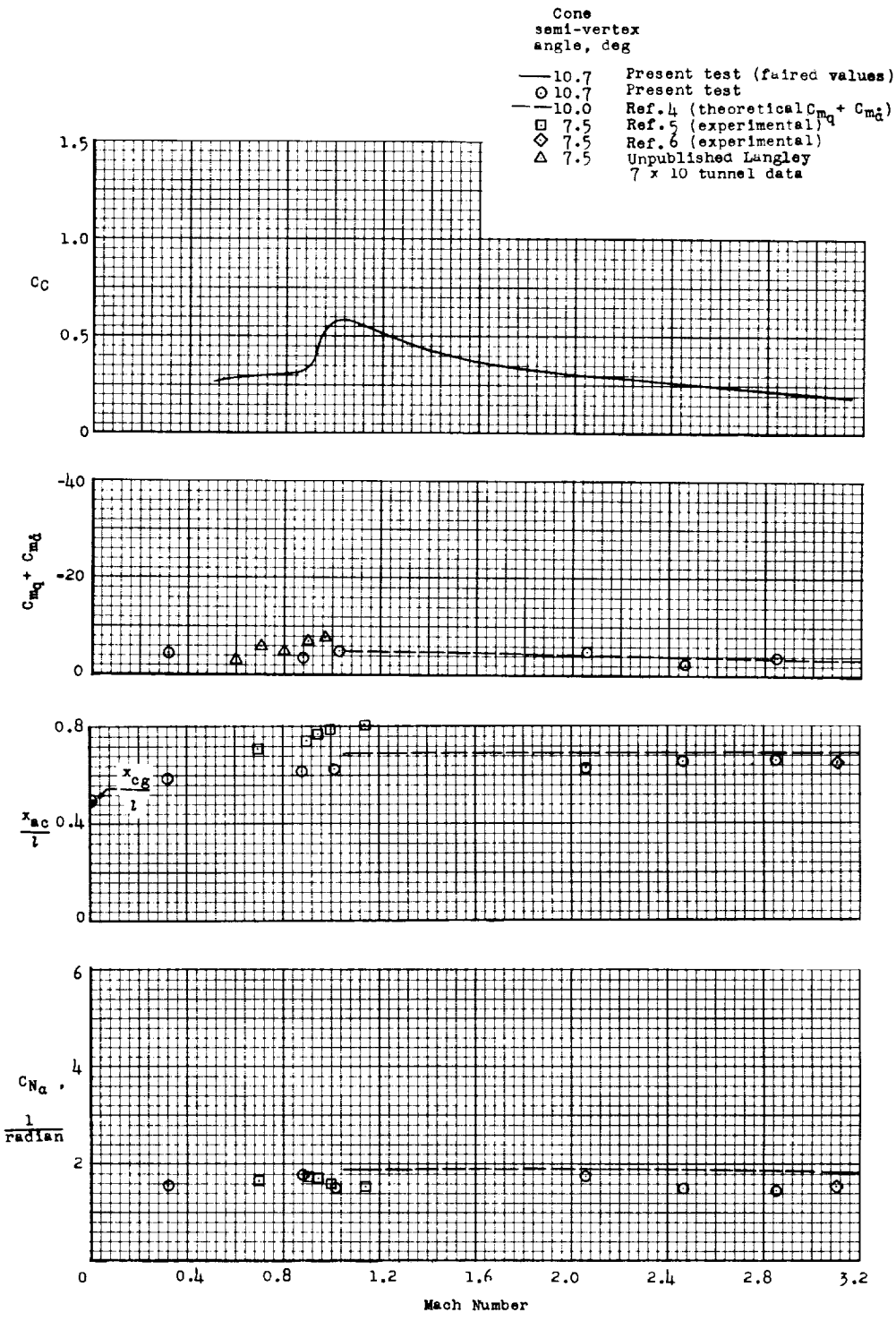

Figure 12.- Aerodynamic characteristics of the cone model.

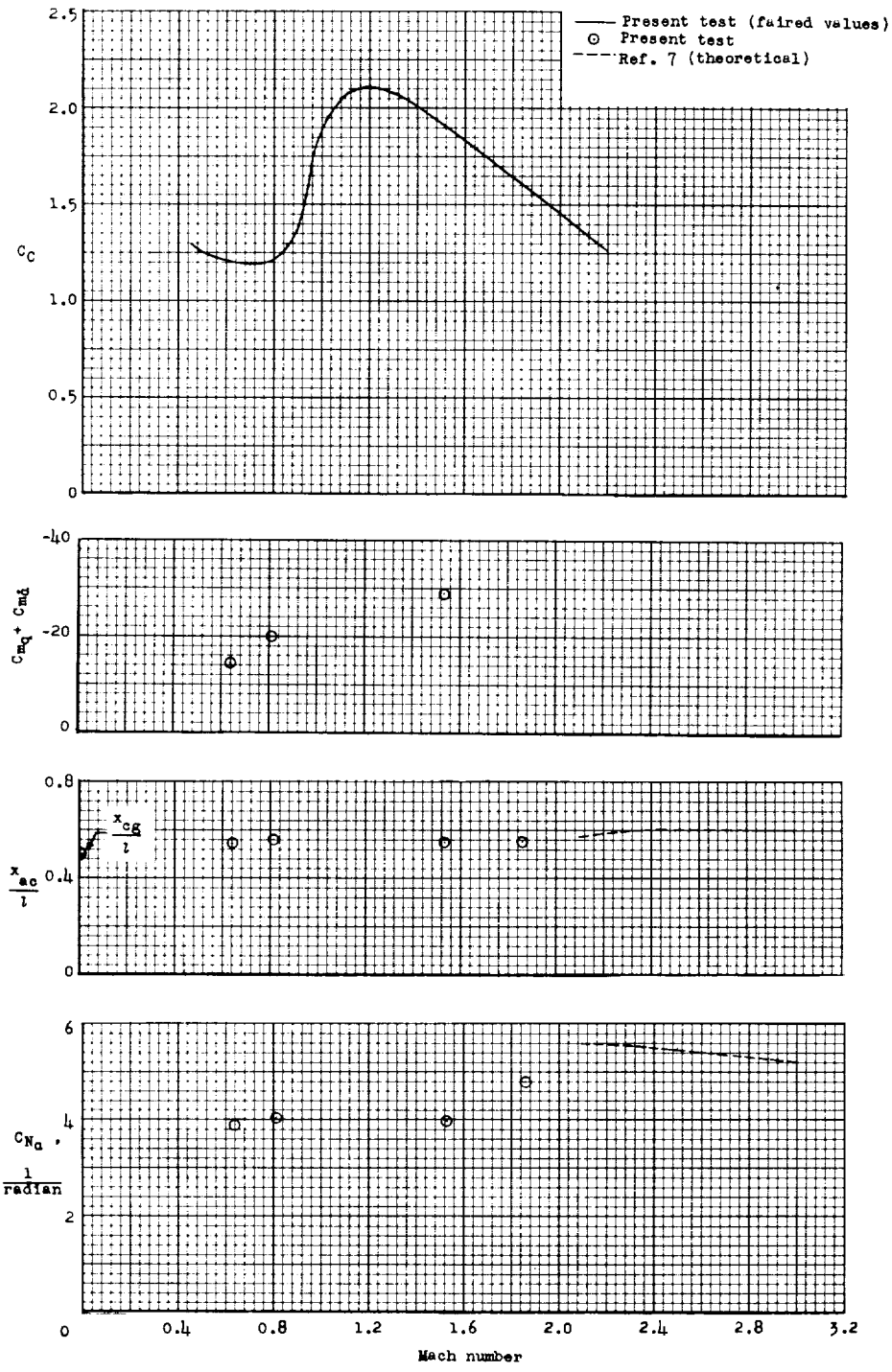

Figure 13.- Aerodynamic characteristics of the ogive model.